20th Australasian Fluid Mechanics Conference
Perth, Australia
5-8 December 2016

A Numerical Model of Microfluidic Inertial Separation

Danielle S. Tan[1] **and Shireen Goh**[2]

[1]Department of Mechanical Engineering
National University of Singapore, Singapore 117575

[2]Animal Cell Technology
Bioprocessing Technology Institute, Singapore 138668

Abstract

Microfluidic inertial separation is a technique commonly used to separate out biological cells used in various medical applications. This is typically done by running a cell-water mixture through a channel which spirals outwards, thus causing the mixture to experience gravitational, inertial and viscous drag forces. The resulting flow exhibits the typical Poiseuille velocity profile in the streamwise direction, as well as the circulating velocity field characteristic of Dean's secondary flow profile in the cross-stream plane. The balance of forces causes the cells to move towards an equilibrium position on the inner wall, and is thus easily filtered out. However, when the cell density is increased to above 6×10^7 cells/mL, outer wall focusing is observed in rectangular channels. This is not predicted by any present fluid dynamic theory, and neither can commercial CFD packages simulate it. Our current hypothesis is that this change in equilibrium position is likely to be due to the flow changing from largely cell-fluid interactions to one dominated by cell-cell interactions as the initial concentration of the mixture increases. In this paper we present the preliminary version of a numerical model of a rectangular channel section, developed with the aim of investigating the dynamics of the focusing process – particularly when the initial concentration of cells is varied. We use the discrete element method (DEM) to model the movement of individual cells in a small section of the channel. Particle-scale information including the relative positions, velocities and forces on the simulation particles are tracked as the mixture evolves over time. We compare the simulation results to physical experiments, and find that this preliminary numerical model is promising, but still requires further improvement to accurately reproduce the observed final equilibrium state, particularly the Dean's flow that is crucial in the focusing process.

Introduction

Microparticles are involved in many applications in the biochemical and biomedical industries, and thus greater focus has been placed on micro-scale processes. One such process is filtration of biological cells from a fluid-cell mixture [6, 10, 13, 17], also known as microfluidic filtration, or microfluidic cell sorting. There have been many proposals and improvements to the filtration technique, utilising inertial forces by passing the fluid-cell mixture through an outwardly-spiraling channel [1, 2, 4, 9, 12, 14, 19]. These include both physical [1, 2, 12, 14, 19] and numerical experiments [5, 9, 11, 15]. The main idea behind these is that as the fluid moves through the channel, it experiences gravitational, inertial and viscous drag forces, finally resulting in the typical Poiseuille velocity profile in the streamwise direction, as well as the circulating velocity field characteristic of Dean's secondary flow profile in the cross-stream plane [4, 12, 18]. Due to the balance of inertial and lift forces present in the spiral channels, the cells move towards an 'equilibrium' location relative to the channel cross-section. The channel outlet can then be split appropriately such that the fluid and the cells leave via separate outlets. For the trapezoidal channels currently reported in literature, the cells typically move towards the outer wall (known as 'outer wall focusing'), and has been speculated to be caused by the skewed Dean's secondary flow profile.

Recent empirical results achieved at the Bioprocessing Technology Institute (Singapore) have exhibited a filtration efficiency of 98.2% for a cell density of 10^8 cells/mL [8], higher than the (to-date) best performing device reported by [17] which has an efficiency of 74.8%. In addition, observations were made that as the cell density was increased from low to high densities, the focusing position shifted from the inner wall to the outer wall. This density-dependent behaviour appears to be similar to that observed for granular segregation (unmixing) in a chute, whereby the direction of segregation changed depending on whether the initial mixture had a high or low solid fraction [7]. This leads us to the hypothesis that outer wall focusing is most likely caused by particle-fluid interactions, which may cause a distortion of the Dean's secondary flow profile, and increased particle-particle interactions when the cell density is increased significantly to be considered non-dilute. As such, we believe that we may gain a greater understanding and insight through particle-based numerical simulations, which will allow us to obtain particle-scale information such as inter-particle forces.

In this paper we present the preliminary numerical model used for this simulation: first an overview of the Discrete Element Method (DEM), the chosen numerical method; followed by a description of the layout of the numerical simulation; and finally an evaluation of this version of the simulation.

Overview of Discrete Element Method

The Discrete Element Method (DEM) was first proposed in 1979 by Cundall and Strack [3], as a time-marching numerical method meant for collections of particles. It tracks the positions and velocities of every single particle in the system, and updates them at each incremental timestep. For a soft-sphere model – that is, assuming the particles are soft enough that they can be deformed – the relative deformation of particle pairs is used to formulate the forces experienced by each particle. This relationship is known as the contact force model, the simplest form of which is Hooke's Law.

The general procedure at each timestep in a soft-sphere DEM simulation is as follows:

1. For every pair of particles, the relative force on each other is calculated using a contact force model which is a function of their relative position.

2. The total force on each particle is found by summing the relative force contributions from all of its neighbours; any external forces like gravity are also added.

3. Using Newton's laws of motion, the acceleration on each

particle is found. The increment in velocity and displacement is determined by numerical integration.

4. Finally, the set of particle positions and velocities are updated.

The most crucial part of the cycle is, arguably, the contact force model. Many versions can and have been employed, the most popular being a spring-damper combination. In other words the particles are treated as springs, with an associated 'spring stiffness' k which is typically resolved into both a normal component k_n and tangential component k_t. The 'spring deplacement' is given by the particle deformation $\vec{\delta}$, which also has normal and tangential components δ_n and δ_t. Damping is also considered, as a function of the rate of deformation $\dot{\vec{\delta}}$, as a way of dissipating energy.

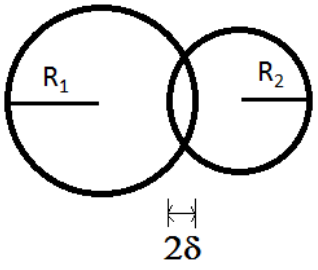

Figure 1: Sketch of two spherical particles with radii R_1 and R_2 respectively, and their deformation δ when in contact.

Figure 1 shows a sketch of two particles in contact, and the resulting deformation experienced by each particle. The deformation is represented by the small overlapping region. There are no exact expressions relating the deformation to the resulting (repulsive) normal and tangential forces, and as mentioned earlier Hooke's Law is one of the versions commonly used. Here we use a nonlinear force contact model based on Hertz-Mindlin contact theory; the magnitudes of the force components are given as:

$$F_n = -k_n\delta_n^{3/2} - \eta_n\delta_n^{1/4}\dot{\delta}_n\,, \tag{1}$$

$$F_t = \min\left\{ \begin{array}{c} -k_t\delta_n^{1/2}\delta_t - \eta_t\delta_n^{1/4}\dot{\delta}_t \\ \mu F_n \end{array} \right. , \tag{2}$$

where F_n and F_t are the normal and tangential components of the force exerted on particle i by particle j in the direction $\vec{x_i j} \equiv \vec{x_i} - \vec{x_j}$ connecting the two particles' centres; k_n, k_t, eta_n and eta_t are the normal and tangential stiffness and damping coefficients corresponding to the pair of particles in contact, and μ is the friction coefficient.

We can relate the stiffness and damping coefficients to material properties like density ρ, mass m, Poisson's ratio ν, Young's modulus E and the shear modulus G. These are shown in table 1. The coefficient α is related to the coefficient of restitution, developed by Tsuji et al. [16].

For our numerical simulation, the three main components are the fluid, the biological cells, and the channel walls. The corresponding material properties used are shown in table 2.

As a fluid, water does not have a Young's modulus. Instead, we estimated this value using $E \approx \rho c^2$, where $c = 1480$ m/s is the speed of sound in water (according to EngineeringToolbox.com, for water at 20°C). The material properties for the channel walls were taken from Solidworks for ABS polycarbonate, and we used the material properties of Chinese hamster ovary cells for the biological cells.

Variable	Formulae
k_n	$(4/3)\sqrt{R_{\text{eff}}}E_{\text{eff}}$
k_t	$8\sqrt{R_{\text{eff}}}G_{\text{eff}}$
γ_n	$\alpha\sqrt{m_{\text{eff}}k_n}$
γ_t	$\alpha\sqrt{m_{\text{eff}}k_t}$
R_{eff}	$\left(\frac{1}{R_1}+\frac{1}{R_2}\right)^{-1}$
E_{eff}	$\left[\frac{1-\nu_1^2}{E_1}+\frac{1-\nu_2^2}{E_2}\right]^{-1}$
G_{eff}	$\left[\frac{2(1+\nu_1)(2-\nu_1)}{E_1}+\frac{2(1+\nu_2)(2-\nu_2)}{E_2}\right]^{-1}$
m_{eff}	$\left(\frac{1}{m_1}+\frac{1}{m_2}\right)^{-1}$

Table 1: Formulae for calculating stiffness and damping coefficients for a pair of particles in contact.

	Cell	Fluid	Walls
ρ (kg/m^3)	1000	1000	1070
ν	0.3	0.5	0.39
E (Pa)	1500	2.2×10^9	2.4×10^9

Table 2: Material properties used for the model fluid, biological cells and channel walls.

Numerical Simulation Setup

The numerical simulation models an intermediate section of the spiral channel, with a rectangular cross-section. Due to patent issues, the exact dimensions of the channel, as well as the input velocity conditions, cannot be released here. Figure 2 shows a sketch of the simulation setup, with the 3D coordinate system. The $x-$ and negative $y-$ directions are cross-stream and streamwise directions respectively.

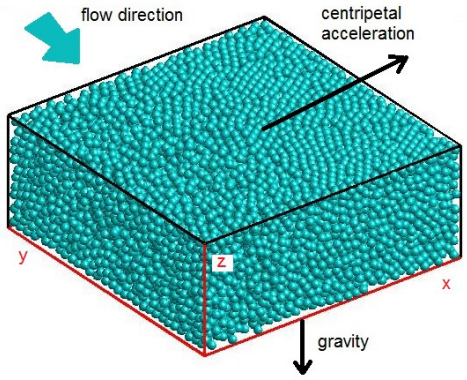

Figure 2: Setup of DEM system: rectangular section with periodic boundary conditions in the x-direction, representing an intermediate section of microchannel. Flow in the channel is in the negative y-direction. External forces applied to the simulation particles are gravity (in negative z-direction), and centripetal force acting in the positive x-direction (towards the centre of the spiral microchannel setup).

Initial Conditions

The particles were initialised in a random arrangement, close to but not exactly a lattice arrangement. A very small initial velocity was given in both the x- and z-directions (i.e. the cross-stream velocity components), while the streamwise velocity component (negative y-direction) was prescribed to be similar to that of a fully-developed Poiseuille flow. The reason for doing so was to reduce computation time, and we feel that this is not an unreasonable simplification. Figure 3 shows the prescribed initial velocity (the magnitudes are again removed for patent reasons). Note that because the velocities shown were calculated by splitting the $x-z$ plane into bins and taking the bin averages, the values are somewhat smoothed.

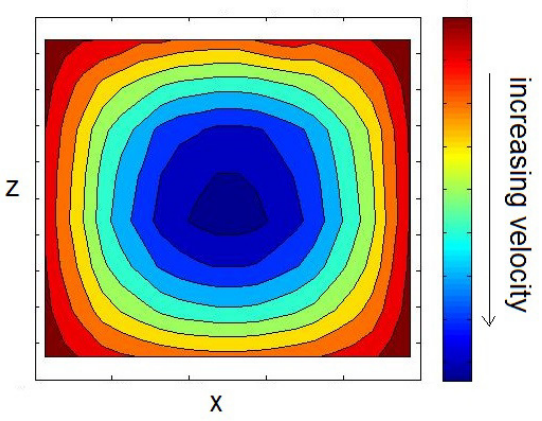

Figure 3: Prescribed initial streamwise velocity, plotted as velocity contours in the $x-z$ plane.

Scaling

In addition to the Poiseuille-like initial conditions, we applied a scaling such that the timestep size could be increased, and thus the total computation time reduced further. This was accomplished by ensuring that (1) the particle Reynolds' number, and (2) the ratio of gravitational to centripetal acceleration, are equal in both the real and simulated systems.

Keeping material properties like the fluid density ρ_f and viscosity μ_f constant, and using subscripts R and S to denote the real and simulation parameters respectively, we have

$$\begin{aligned} \mathrm{Re}_R &= \mathrm{Re}_S \\ \frac{\rho_f V_R d_R}{\mu_f} &= \frac{\rho_f V_S d_S}{\mu_f} \\ \Rightarrow V_S &= V_R \left(\frac{d_R}{d_S}\right) \end{aligned} \tag{3}$$

where d is the average particle diameter and V the particle velocity, and

$$\begin{aligned} \frac{\mathrm{gravity}_R}{\mathrm{centripetal}_R} &= \frac{\mathrm{gravity}_S}{\mathrm{centripetal}_S} \\ \frac{g_R}{V_R^2 d_R^{-1}} &= \frac{g_S}{V_S^2 d_S^{-1}} \\ \Rightarrow g_S &= g_R \left(\frac{V_S}{V_R}\right)^2 \left(\frac{d_R}{d_S}\right) \\ g_S &= g_R \left(\frac{d_R}{d_S}\right)^3 \end{aligned} \tag{4}$$

where g is the gravitational acceleration. From these two scaling relationships, if we scale *up* the particle size by a factor of d_S/d_R, then the velocities in the simulation will be scaled *down* by a factor d_R/d_S, and the gravitational acceleration will be scaled *down* by $(d_R/d_S)^3$.

Preliminary Results

The very first validation test is for the DEM simulation to reproduce the secondary Dean's flow, without the presence of the biological cells. Figures 4-5 show some results from a simulation involving approximately 14000 particles in a domain of size $33 \times 33 \times 13$ particle diameters, after 0.5 s and 2 s of simulated time (5×10^4 and 2×10^5 timesteps respectively), specifically the cross-stream velocity and particle concentration in the $x-z$ plane.

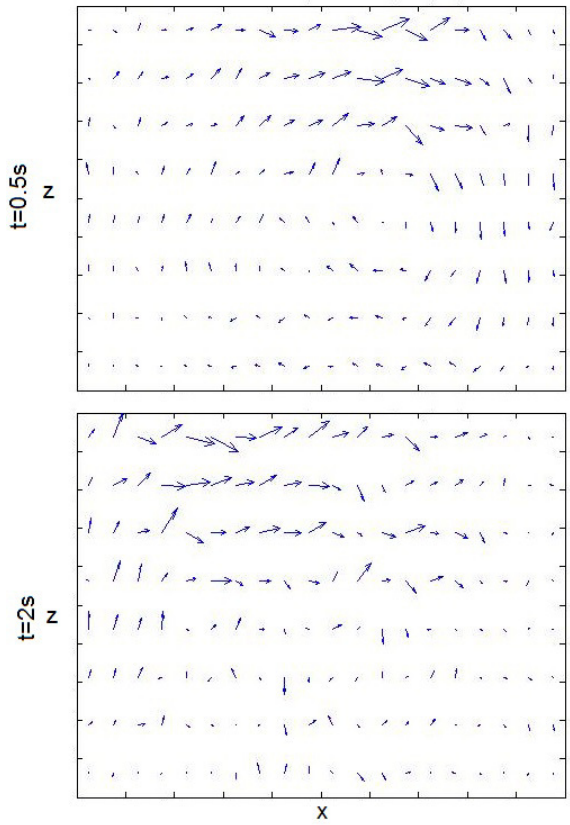

Figure 4: Cross-stream velocity at $t = 0.5$ and $t = 2$ s, plotted as velocity vectors in the $x-z$ plane, for the purely-fluid simulation.

From the physical experiments, the cell focusing typically occurs within 30 s. This means that the secondary Dean's flow should also have formed before then. Thus, the formation of a vortex in figure 4 – the cross-stream velocity profile – within the first 0.5 s is very promising. However this vortex formation dissipates very quickly as seen for $t = 2$ s, which is an indication that the energy is being dissipated too quickly in the system. Additionally, upon looking at figure 5 we see that although the majority of the local concentration is around 0.4 throughout initially, the particles rapidly congregate towards the bottom right of the channel, which implies that the centripetal and gravitational forces are not being balanced by the wall friction.

Qualitatively, these results are independent of the number of particles used in the simulation, but an increasing number (and thus smaller size of) particles would give results that come closer to that of a continuous system.

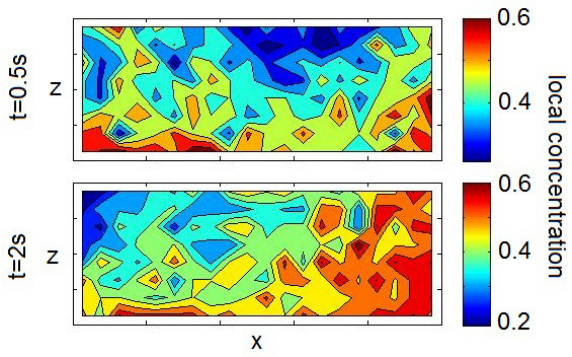

Figure 5: Particle concentration at $t = 0.5$ and $t = 2$ s, plotted as contours in the $x-z$ plane, for the purely-fluid simulation.

Summary

In order to gain a better understanding of the particle interactions that potentially lead to a switch in focusing direction in microinertial separation devices, we propose the use of a Discrete Element Method numerical simulation. The simulation uses spherical particles to represent both the fluid and the biological cells, flowing in a channel of rectangular cross-section which represents an intermediate portion of the physical separation device. The DEM method uses a spring-damper force contact model, which relates the relative overlapping of neighbouring particles to the repulsive force they experience. The stiffness and damping coefficients involved are functions of material properties. For the first validation test we expect to see the secondary Dean's flow developing. This preliminary numerical simulation does exhibit vortex formation, but the damping in the system is too strong, causing the vortex to dissipate quickly. Additionally, wall effect is clearly not strong enough to balance both the centripetal and gravitational forces. As such there is still much room for improvement of the numerical simulation.

References

[1] Bhagat, A.A.S, Kuntaegowdanahalli, S.S. and Papautsky, I., Continuous particle separation in spiral microchannels using dean flows and differential migration, *Lab on a Chip*, **8**, 2008, 1906–1914.

[2] Bhagat, A.A.S., Hou, H.W., Li, L.D., Lim, C.T. and Han, J., Dean flow fractionation (DFF) isolation of circulating tumor cells (CTC) from blood, in *15th International Conference on Miniaturized Systems for Chemistry and Life Sciences*, 2–6 Oct 2011, Seattle, Washington, U.S..

[3] Cundall, P.A. and Strack, O.D.L., A discrete numerical model for granular assemblies, *Géotechnique*, **29**(1), 1979, 47–65.

[4] Di Carlo, D., Irimia, D., Tompkins, R.G. and Toner, M., Continuous inertial focusing, ordering and separation of particles in microchannels, *Proceedings of the National Academy of Sciences of the United States of America*, **104**(48), 2007, 18892–18897.

[5] Di Carlo, D., Edd, J.F., Irimia, D., Tompkins, R.G. and Toner, M., Equilibrium Separation and Filtration of Particles Using Differential Inertial Focusing, *Analytical Chemistry*, **80**(6), 2008, 2204–2211.

[6] Di Carlo, D., Inertial microfluidics, *Critical Review*, **9**, 2009, 3038–3046.

[7] Fan, Y. and Hill, K.M., Phase transitions in shear-induced segregation of granular mixtures, *Phys. Rev. Lett.*, **106**(218301), 2011.

[8] Goh, S., Tan, S.M., Tan, D.S. and Yang, Y.S., New Phenomenon: Outer Wall Focusing at High Cell Densities Enables High Performance Cell Microfilter at Low Shear Stress, in *The 20th International Conference on Miniturized System for Chemistry and Life Sciences (MicroTAS)*, 9–13 Oct 2016, Dublin, Ireland. (Poster)

[9] Guan, G., Wu, L., Bhagat, A.A.S, Li, Z., Chen, P.C.Y., Chao, S., Ong, C.J. and Han, J., Spiral microchannel with rectangular and trapezoidal cross-sections for size based particle separation, *Scientific Reports*, **3**(1475), 2012, 1–9.

[10] Karimi, A., Yazdi, S. and Ardekani, A. M., Hydrodynamic mechanisms of cell and particle trapping in microfluidics, *Biomicrofluids*, **7**(021501), 2013, 1–24.

[11] Lee, D.J., Brenner, H., Youn, J.R. and Song, Y.S., Multiplex Particle Focusing via Hydrodynamic Force in Viscoelastic Fluids, *Scientific Reports*, **3**(3258), 2013, 1–8.

[12] Nivedita, N., Ligrani, P. and Papautsky, I., Evolution of secondary Dean vortices in spiral microchannels for cell separations, in*17th International Conference on Miniaturized Systems for Chemistry and Life Sciences*, 27–31 Oct 2013, Freiburg, Germany.

[13] Pamme, N., Continuous flow separations in microfluidic devices, *Critical Review*, **7**, 2007, 1644–1659.

[14] Russom, A., Gupta, A.K., Nagrath, S., Di Carlo, D., Edd, J.F. and Toner, M., Differential inertial focusing of particles in curved low-aspect-ratio microchannels, *New J. Phys.*, **11**(075025), 2009, 1–11.

[15] Sun, J., Li, M., Liu, C., Zhang, Y., Liu, D., Liu, W., Hu, G. and Jiang, X., Double spiral microchannel for label-free tumor cell separation and enrichment, *Lab Chip*, **12**, 2012, 3952–3960.

[16] Tsuji, Y., Tanaka, T. and Ishida, T., Lagrangian numerical simulation of plug flow of cohesionless particles in a horizontal pipe, *Powder Tech.*, **71**, 1992, 239–250.

[17] Warkiani, M., Wu, L., Tay, A.K.P. and Han, J., Large-Volume Microfluidic Cell Sorting for Biomedical Applications, *Annu. Rev. Biomed. Eng.*, **17**, 2015, 1–34.

[18] Yang, B.H., Wang, J., Joseph, D.D., Hu, H.H., Pan, T.-W. and Glowinski, R., Migration of a sphere in tube flow, *J. Fluid Mech.*, **540**, 2005, 109–131.

[19] Zhang, J., Yan, S., Sluyter, R., Li, W., Alici, G. and Nam-T.N., Inertial particle separation by differential equilibrium positions in a symmetrical serpentine micro-channel, *Scientific Reports*, **4**(4527), 2014.